This article has been accepted for publication in a future issue of this journal, but has not been fully edited. Content may change prior to final publication. Citation information: DOI 10.1109/TAP.2017.2775286, IEEE Transactions on Antennas and Propagation



# Ultrawideband Lossless Cavity-Backed Vivaldi Antenna

Elie G. Tianang, *Student Member, IEEE*, Mohamed A. Elmansouri, *Senior Member, IEEE*, and Dejan S. Filipovic, *Senior Member, IEEE*

***Abstract*— An ultrawideband, lossless cavity-backed Vivaldi antenna array for flush-mounting applications is proposed. Eigenmode analysis, used to investigate antenna-cavity interaction, has shown that the entire structure may resonate within the band of interest resulting in a significant degradation of antenna performance. A simple approach based on connecting the array's edge elements in E-plane to the cavity walls is utilized to eliminate the deleterious impact of these cavity resonances. The proposed antenna is a 3×4 array with 3 elements in E-plane and 4 elements in H-plane, fabricated using stacked all-metal printed circuit board technique. Resonant-free behavior with gain better than 5dBi and VSWR < 2 from 1.5 to 7.5 GHz is obtained. High-quality radiation patterns with side lobe levels lower than 20dB over the same bandwidth are also demonstrated. Scan performance of the proposed cavity-backed antenna is investigated in two principal planes and is shown to have similar performance compared to its free-standing counterpart.**

***Index Terms*—Cavity-backed antennas, flush-mountable antennas, phased arrays, tapered-slot antennas, ultra wideband antennas, Vivaldi antennas.**

## I. Introduction

With the increased demand for advanced wireless communications in airborne systems, there is a growing need for single aperture antennas with multiple functionalities in both, RF, and mechanical domains. From mechanical perspective, antennas are required to be compact given the limited space available and flush mountable to conform to the aerodynamics of the platform. In RF domain, it is desired that antennas have wide bandwidth, low loss, and some scanning ability. In recent years, tightly coupled arrays have been considered for such RF demands [1]-[5]. A close separation between elements is used therein to increase scanning bandwidth. Since Munk's used wire array elements to describe the principle of operation of this class of radiators [6], different unit-cell elements have been researched including dipoles [2], bowtie [3], patch [7], and Vivaldi [8], just to name a few. A photograph of a Vivaldi array, discussed in this paper, is shown in Fig. 1 where its ultrawideband capabilities

This work is supported by the Naval Research Lab (NRL) under contract #N00173-15-C-2021.

The authors are with the Department of, Electrical, Computer, and Energy Engineering, University of Colorado, Boulder, CO 80309-0425 (e-mail: {elie.tianang,mohamed.elmansouri,dejan.filipovic}@colorado.edu).

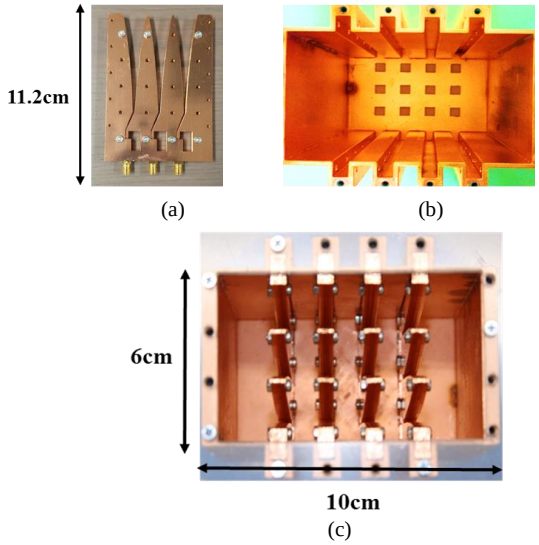


Fig. 1. Photograph of the prototyped cavity-backed 3×4 Vivaldi antenna array: (a) single row of the array, (b) 3D-printed and copper plated rectangular cavity showing the longitudinal groove reserved for each row of the array, and (c) fully –assembled array recessed in the cavity.

are extended to a more robust cavity-back embodiment. As seen, the entire antenna is developed to be all-metal. A design approach similar to an all-metal aluminum block proposed in [9] is followed. It is important to note that the works discussed in [9] and in most planar based tightly coupled Vivaldi arrays [8], [10], focus mainly on wide scan angle applications and are based on arrays with more than 30 elements. These arrays are not designed to be flush-mounted in a compact way and are usually backed by a large ground plane. While this ground plane may be used to mitigate back radiation, the exposed profile of the antenna is an issue for its practical use when aerodynamic and conceal needs are important. The cavity-backed array shown in Fig.1 ensures flush mounting capability and easy concealment.

A design of an ultrawideband cavity-backed antenna is challenging given the deleterious impact of high quality factor (Q) cavity resonances on antenna performance. Lossy materials such as absorbers are often placed near the surface of the cavity to dampen these high-Q resonant modes [11]. This; however, can lead to a degradation of antenna efficiency. Another approach often used is to increase the separation between the antenna and the cavity in order to reduce their res-

This article has been accepted for publication in a future issue of this journal, but has not been fully edited. Content may change prior to final publication. Citation information: DOI 10.1109/TAP.2017.2775286, IEEE Transactions on Antennas and Propagation



TABLE I
COMPARISON BETWEEN CAVITY-BACKED VIVALDI ANTENNAS

| Ref. | Size ($Area \times H$) | BW ($GHz$) | Cavity description |
|---|---|---|---|
| This work | $0.15\lambda_{1.5GHz}^2 \times 0.55\lambda_{1.5GHz}$ | 1.5-7.5 | Lossless, rectang., closed |
| [15] | $0.26\lambda_{2GHz}^2 \times 0.73\lambda_{2GHz}$ | 2-11 | Diel.-loaded, open base |
| [16] | $0.18\lambda_{2GHz}^2 \times 0.73\lambda_{2GHz}$ | 2-8 | Foam-loaded |
| [18] | $1.6\lambda_{18GHz}^2 \times 1.98\lambda_{18GHz}$ | 18-45 | Absorb.-loaded |

pective coupling [12]-[14]. This is done at the expense of an increased overall size; thereby deflating a wider use of these antennas and arrays.

Only few design attempts of a flush-mounted Vivaldi antenna are reported in open literature [15]-[18]. In [15], a Vivaldi element is placed in a cylindrical cavity; yet, the bottom of the cavity is kept open to eliminate cavity modes. However, this approach makes the RF isolation of backend electronics nearly impossible. In [16], the size and the shape of a trapezoidal cavity is increased to mitigate its interaction with the antenna within the operating bandwidth leading to a relatively large, non-compact, flush-mountable structure. In, [17], only the feed region is backed with a cavity leaving the radiating section free-standing. A circular cavity loaded with absorber is presented in [18] for receive-only direction finding. While this antenna may be suitable for receiving applications, the reduction in efficiency is not acceptable for prime power needy RF uses. A comparison between these antennas and the cavity-backed array proposed in this paper is shown in Table. I. As seen, none of the reported designs combines compact form factor, nearly lossless and resonant free behavior as demonstrated herein.

In this paper, a design approach that led to a resonant free Vivaldi antenna array fully recessed inside a lossless metallic cavity, is proposed. Initial investigation of this antenna is reported in [19]-[20]. In [19], corrugated surfaces combined with absorbers are used to mitigate cavity resonances leading to reduction in antenna efficiency. In [20], a summary of the proposed antenna performance is presented without details aimed to understand the actual physical impact of the cavity including resonances. Also, the design procedure and scanning capability for the proposed antenna are not discussed in [20].

In this paper, a parametric study is performed to evaluate effects of the antenna proximity to the side walls in two principal planes. Eigenmode analysis is used to study antenna-cavity interaction in both E- and H-planes. The proposed 3×4 array is fabricated using a multilayer stacked all-metal circuit board technique [21]. The scan performance of the fabricated array is investigated using the measured active element patterns. The paper is organized as follows: the unit-cell and array design are presented in Section II, whereas the detailed fabrication process is discussed in Section III. In Section IV, the robustness of the design is assured by comparing theory with experimental data. Discussion Section V overviews scanning capabilities and elaborates on the comparison with a free-standing embodiment.

## II. ANTENNA DESIGN AND ANALYSIS

### A. Antenna Design

The geometry of the unit-cell and its parameters are shown in Fig. 2 and Table II. To maintain low side-lobe level (SLL) over the 1.5 – 7.5GHz bandwidth (chosen for the purpose of this work; but electromagnetic scaling can be applied for other ranges), the unit-cell width $W$ is chosen to be $18mm$ ($< \lambda_{8GHz}/2$). To enable easy attachment of a coaxial connector, the thickness of the element is chosen to be $6mm$ ($\lambda_{1.5GHz}/33$). The advantages of a thick Vivaldi antenna have been previously reported in [22]. The feed region of the unit-cell, including the transition from the coax to the slotted section of the element is highlighted in Fig. 2. Also shown is the slotted section of the unit-cell which is seen to be better assimilated to a parallel plate waveguide given its thickness. The width $i$ between the two plates is chosen for a $50\Omega$ characteristic impedance. To reduce the discontinuity at the coax to parallel plate transition, a $50\Omega$ air-filled rectangular coaxial line is implemented [23]. This transition is further improved by equating the plate thickness to the width of the inner conductor of the rectangular coaxial line.

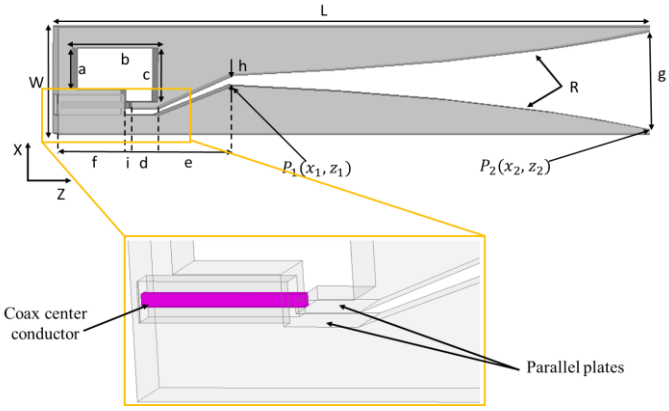


Fig. 2. Unit-cell of the proposed array with characteristic parameters denoted. Also shown is the magnified feed region clearly denoting the coaxial to parallel plate transition.

TABLE II
DESIGN PARAMETERS OF ARRAY UNIT-CELL (IN MM)

| Parameter | $a$ | $b$ | $c$ | $d$ | $e$ | $f$ |
|---|---|---|---|---|---|---|
| Value | 8 | 14 | 11 | 5.13 | 13.97 | 12.54 |
| Parameter | $g$ | $h$ | $i$ | $W$ | $L$ | $R$ |
| Value | 17 | 1.72 | 1.1 | 18 | 112 | 0.2 |

Other parameters are determined based on an infinite array analysis [24] aimed to achieve wideband impedance match at the reduced computational cost [9]. It is found that the main parameters affecting VSWR are the exponential growth rate ($R$), the length ($L$), and the open cavity delimited by segment ($a - b - c$) shown in Fig. 2. The impedance match bandwidth is increased with increase in the length $L$ which is chosen to be $\sim \lambda_{1.5GHz}/2$, to keep the overall profile of the array low. The exponential taper is described as,

This article has been accepted for publication in a future issue of this journal, but has not been fully edited. Content may change prior to final publication. Citation information: DOI 10.1109/TAP.2017.2775286, IEEE Transactions on Antennas and Propagation



$$x = R_1 e^{Rz} + R_2 \quad (1)$$

where

$$R_1 = \frac{x_2 - x_1}{e^{Rz_2} - e^{Rz_1}} \quad (2)$$

$$R_2 = \frac{x_1 e^{Rz_2} - x_2 e^{Rz_1}}{e^{Rz_2} - e^{Rz_1}} \quad (3)$$

and $0 \leq R \leq 1$ with 0 being a linear taper.

Values of $R$ close to zero increase gain at lower frequencies. When $R = 0$, the discontinuity between the feed and the flare section is increased, leading to the degradation in impedance match. Increasing the size of the open cavity improves the match at low frequencies; however, its fundamental resonant frequency is lowered. The size of this cavity is adjusted to have its fundamental resonant frequency above 7.5GHz.

The active VSWR of a tightly coupled infinite array composed of unit-cells with parameters from Table II is shown in Fig. 3. The infinite array response is used to guide the selection of a finite 3×4 free-standing array also shown in the same figure. The computed VSWR of this 3×4 array fed with ideal 12-way power divider is plotted in Fig. 3. As seen, the VSWR<2 is obtained above 2.5GHz therefore verifying the usefulness of parametric studies conducted with infinite array. As expected, the infinite array has better match at lower frequencies. The finite array approaches the infinite array model as the number of elements is increased; however, the 3×4 array is chosen as compromise between the size, desired minimum gain of 5dBi, and turn-on frequency of 1.5GHz.

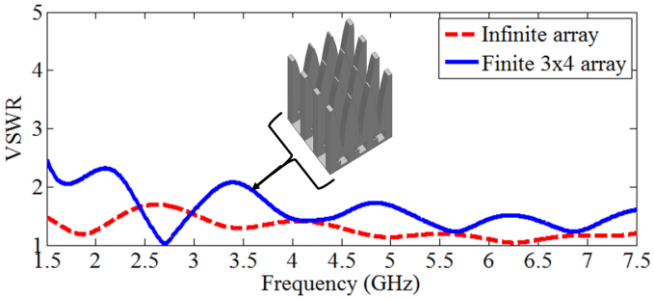


Fig. 3. Active VSWR of an infinite and finite 3×4 Vivaldi arrays. The 3×4 array is fed using ideal 12-way power divider in this analysis.

### *B. Antenna Analysis*

Effect of recessing the designed 3×4 Vivaldi array in a rectangular metallic enclosure, as illustrated in Fig. 4, is analyzed in this Section. The bottom side of the array is connected to the cavity base. Offset distances, $D_x$ and $D_y$, are kept between the array and the cavity side walls in H- and E-plane, respectively. The center-to-center separation between the array elements in H-plane, $D_s$, is kept equal to the unit-cell width $W$ to maintain low side-lobe level in the H-plane cut. Cavity height is kept equal to the unit-cell length $L$. Three elements are connected in E-plane to form a single row of the array. The values of $D_x$ and $D_y$ are varied and the cavity-backed array performance is analyzed.

Offset distance $D_x$ is set respectively to 0, 1, 5, and 40mm while keeping $D_y$ = 20mm. A zero offset means a direct connection between the array and the cavity walls, while offset values equal to 1mm and 40mm are used to investigate respectively strong and weak interaction with the cavity. The simulated VSWR and broadside gain of the uniformly excited

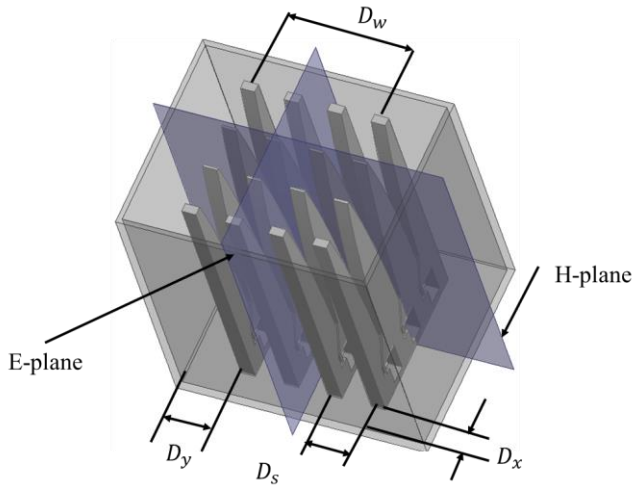


Fig. 4. Geometrical arrangement of the recessed 3×4 array antenna inside a cavity with depicted E- and H- planes.

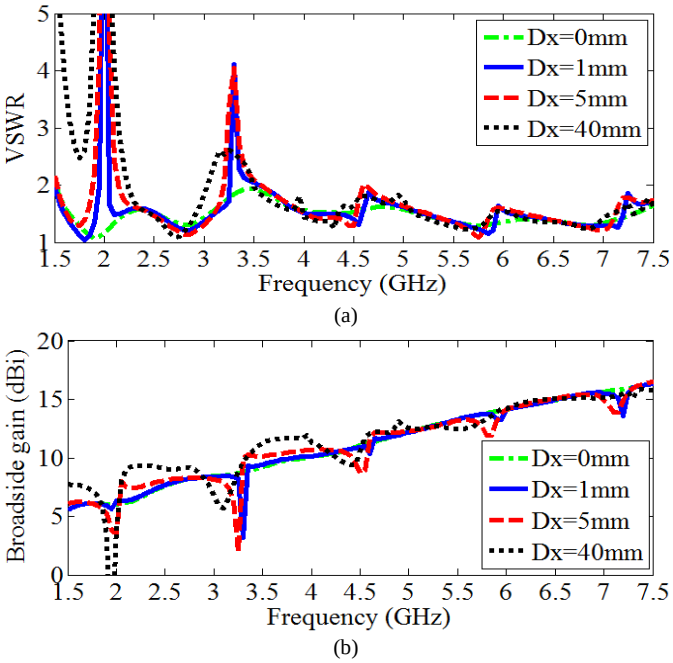


Fig. 5. (a) VSWR, and (b) Broadside gain of the 3×4 Vivaldi array recessed in a cavity with varying separation between the H-plane wall and the cavity.

cavity-backed array are shown in Fig. 5 for different values of $D_x$. As seen, periodic dips in broadside gain correlated with spikes in VSWR are observed at specific frequencies for nonzero value of $D_x$. As $D_x$ keeps increasing the spikes get broader. In this work, the interest is in a compact design where the cavity is brought closer to the antenna.

To better understand these phenomena, the surface currents on the H-plane cavity wall (cavity wall parallel to array H-plane) are plotted in Fig. 6(a) at 1.95GHz, 2.35GHz, 3.2GHz, and 4.45GHz for $D_x$ = 5mm. As seen, standing waves patterns

This article has been accepted for publication in a future issue of this journal, but has not been fully edited. Content may change prior to final publication. Citation information: DOI 10.1109/TAP.2017.2775286, IEEE Transactions on Antennas and Propagation



are clearly formed at 1.95GHz, 3.2GHz, and 4.45GHz. It is observed that the surface current at 2.35GHz is different and does not reveal a standing wave, suggesting that the spikes observed in the gain and VSWR plots are due to the established standing waves at these frequencies.

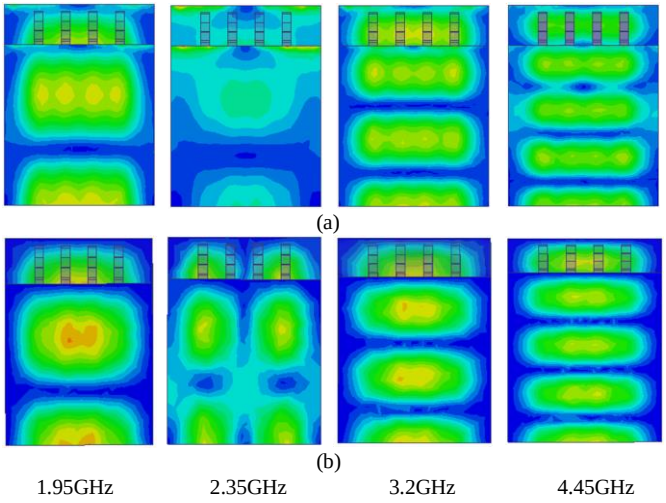


Fig. 6. Surface currents on the H-plane cavity wall when $D_x = 5mm$ obtained with (a) driven, and (b) eigen analysis methods.

To determine the origin of the standing waves at frequencies shown in Fig. 6(a), eigenmode analysis is performed using ANSYS HFSS [25]. It is observed that with perfect magnetic conductor (PMC) boundary placed at the aperture, only a little effect is seen on a driven solution with standing waves described above still present at the same frequencies. The PMC boundary is therefore used to model the cavity aperture in the eigen-value problem. Setting $D_x$ to 5mm, the eigenmode analysis is shown to reveal several resonant modes in the desired band. The surface currents on the H-plane cavity wall are shown in Fig. 6(b) for the resonant modes at 1.98GHz, 3.3GHz, 2.35GHz, and 4.64GHz. As seen, these cavity modes have similar surface current distribution to currents shown in Fig. 6(a) when the array is uniformly excited. The establishment of the standing waves and thus the gain and VSWR deterioration can therefore be attributed to the excitation of these undesired resonant modes. It can further be seen that the driven mode current distribution at 2.35GHz is different to the eigen-current at the same frequency which implies that this resonant mode is not excited by the array.

The eigenmode analysis above is used to confirm the resonance behavior of the antenna at some frequencies but it does not explain why these specific modes are excited. It is found that the cavity E-plane wall, located at $D_y = 20$mm for the purpose of this analysis has no impact on the discussed resonance behavior. To demonstrate this, the broadside gain of the open boundary array (E-plane cavity wall removed) is shown in Fig. 7. As seen, the similar response as in Fig. 5(b) is obtained. It therefore appears that the cavity resonances are excited by another resonating structure. The surface currents at 4.6GHz for this configuration are shown in Fig. 8. As seen, the standing waves are mainly localized at the edge elements, specifically at the gap between these edge elements and the H-plane cavity wall. A magnified view of this section of the antenna with a single row represented is shown in Fig. 9. Given that currents flowing on the edge elements are seen to be localized mainly at the outer boundary, the edge elements can be replaced by a thin strip without perturbing its current distribution. The combination of this strip, the air gap and the cavity wall forms a quasi TEM microstrip line; the ground plane being represented by the cavity wall, and an air dielectric materialized by the gap $D_x$. This line, shorted at the bottom by the cavity base and open at the top, resonates and its resonant frequency is calculated as:

$$f_{res} = (2n+1)c/4L \qquad (4)$$

where $c$ is the speed of light, $L$ is the length of the antenna as denoted in Fig. 2, and $n$ is the order of resonance modes.

The resonant frequencies calculated using (4) and given in Table III are seen to be nearly identical to the frequencies at which spikes are occurring.

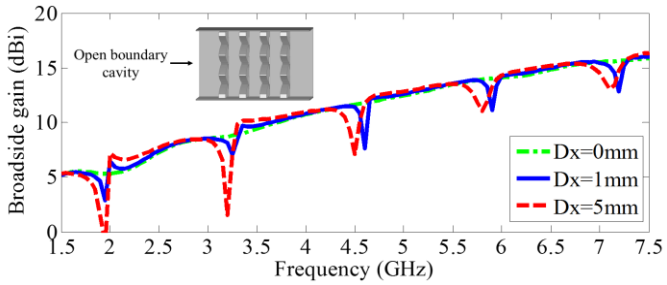


Fig. 7. Broadside gain of the 3×4 Vivaldi array inside an open boundary cavity, as shown in the inset.

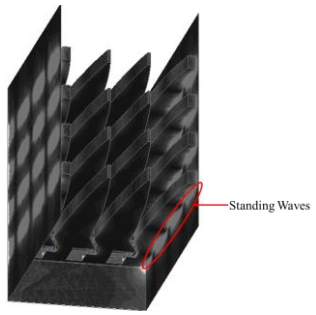


Fig. 8. Surface currents on the H-plane cavity wall when $D_x$ =1mm for the open boundary array.

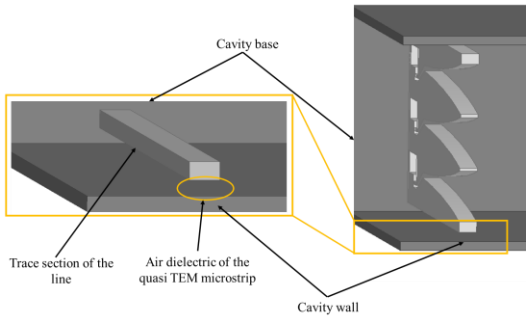


Fig. 9. Illustration of the interface between array edge elements and the cavity as a quasi TEM microstrip line.

This article has been accepted for publication in a future issue of this journal, but has not been fully edited. Content may change prior to final publication. Citation information: DOI 10.1109/TAP.2017.2775286, IEEE Transactions on Antennas and Propagation



TABLE III
ANALYTICAL (CAL) AND FULL-WAVE SIMULATED (SIM) RESONANT FREQUENCIES (IN GHZ)

| n | 0 | 1 | 2 | 3 | 4 |
|---|---|---|---|---|---|
| $f_{res}(cal)$ | 0.67 | 2.08 | 3.34 | 4.68 | 6.02 |
| $f_{res}(sim)$ | | 1.95 | 3.2 | 4.5 | 5.9 |

From this analysis, it can be concluded that the space between the array edge elements and cavity wall provides a transmission line medium for the currents to flow. Resonance occurs as these currents bounce back and forth after seeing an open circuit at the aperture and short circuit at the cavity base. At lower frequencies, currents are weakly radiating before reaching the aperture therefore resulting in a stronger interaction with the cavity. This combination of strong cavity interaction and low radiation results in high Q resonant modes as observed in the VSWR at 1.95GHz in Fig. 5(a). At higher frequencies, more currents radiate before reaching the aperture resulting in the reduced Q.

To mitigate the negative impact of these resonances, two approaches are investigated. First, the resonator section of the antenna is resistively loaded. The gain and VSWR are shown in Fig. 10(a) and Fig. 10(b) for 50Ω and 150Ω respectively. This two values are chosen to assess the effect of low and high resistances. As seen, resonances are eliminated and resistors dissipate part of the reflected currents, therefore contributing to the improved impedance match at low frequencies as seen in Fig. 10(b). Computed antenna efficiency is 78% at 2GHz and over 90% above 3.5GHz. While this reduction in efficiency is acceptable for most receiving applications, it is undesired for transmitting when DC energy resources are scarce.

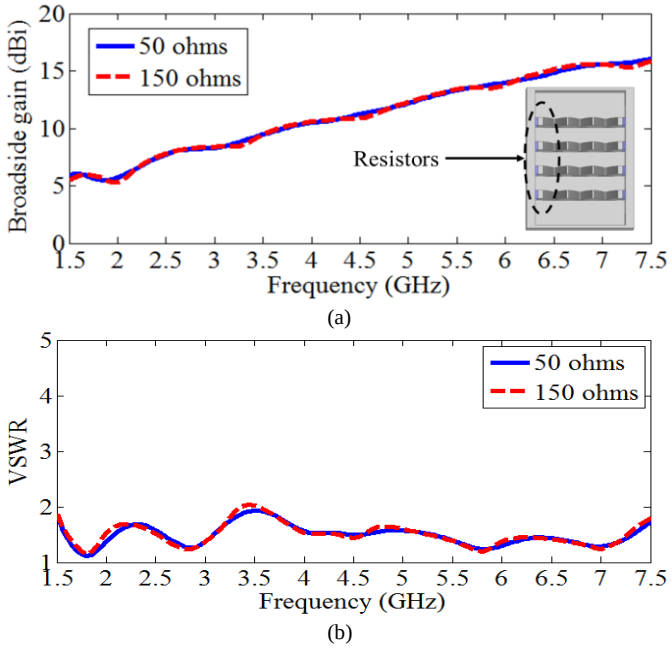


Fig. 10. Performance of the 3×4 cavity-backed Vivaldi array with edge elements terminated with resistors: (a) broadside gain, and (b) VSWR.

The objective of the second approach for mitigating the impact of resonances is to eliminate their topology related origin. These resonances exist due to the gap between the array edge elements and cavity. This gap is eliminated by shorting the array edge elements to the cavity and therefore means for establishing standing waves on that cavity wall are eliminated. Interestingly, this approach is the exact opposite of common techniques relying on recessing linearly polarized antenna in a metallic enclosure [12]-[14]. Rather than increasing the separation between the antenna and the cavity, the E-plane wall of the antenna should be shorted to the cavity. The second approach does not need resistive termination and is adopted in this work.

For complete analysis, the interaction with the E-plane cavity wall is investigated next. To do so, $D_x$ is kept at zero as it is shown to yield better response and $D_y$ is swept from 10 to 20mm with a step of 5mm. The VSWR and broadside gain response for uniformly excited array are shown in Fig. 11.

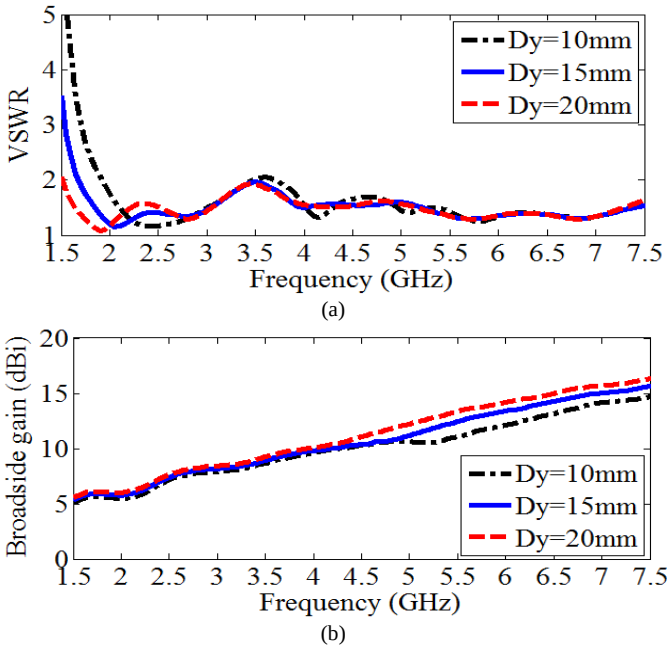


Fig. 11. (a) VSWR, and (b) Broadside gain of the 3×4 Vivaldi array recessed in a cavity with varying separation between the E-plane wall and the cavity.

As seen, E-plane separation does not reveal any noticeable resonance. Nonetheless the E-plane separation is critical in determining the turn on frequency as seen in VSWRs of Fig. 11(a). The separation $D_y$ should be high enough to achieve the desired turn-on frequency and minimum gain, but small enough to mitigate the excitation of high order waveguide modes. To maintain a gain >5dBi and a turn on frequency at 1.5GHz, $D_y$ is set to 20mm.

## III. ARRAY FABRICATION

The 3×4 Vivaldi array and the cavity are fabricated separately using cost-effective manufacturing techniques. Individual rows of the array are assembled by stacking seven printed circuit boards (PCB) to form the geometry as shown in Fig. 12. The utilized PCB stacking process allows the thin inner plate of the coax to parallel plate transition to be easily

machined compared to the conventional CNC-machining. When all the 0.85mm-thick boards are stacked together, the total row thickness is about 6mm as shown in Table. I. Boards 1, 2, 6, and 7 form the bottom and top layers. They are also used to form the bottom and top walls of the rectangular coaxial line, whereas boards 3 and 5 form the side wall. Board 4 is the middle layer and contains the center conductor of the rectangular coax. This central conductor is soldered to the center conductor of a surface mount SMA connector as shown in Fig. 12. Once the connectors are attached to the antenna, the top 3 layers are added to complete the fabrication of a single row. The seven boards are held together using screws as shown in Fig. 1(a) where an assembled row is presented. The rectangular cavity shown in Fig. 1(b) is fabricated using additive manufacturing and plated with a 1.5 oz copper layer. Rectangular holes at the bottom of the cavity are added to enable mounting of SMA connectors (Fig. 12). The flush-mountable array is finally obtained by fixing each row into the groove space available in the rectangular cavity as shown in Fig. 1(c).

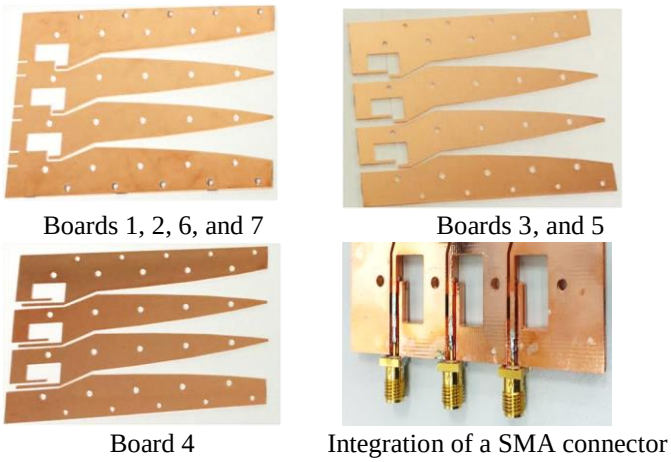


Fig. 12. Illustration of the assembly for the array row: Boards 1,2,6, and 7 form the bottom and top layers. Boards 3 and 5 are used to form the sidewall of the rectangular coaxial line. Board 4 is the center layer and is used to solder the inner conductor of the coaxial feed line.

## IV. Performance

The measured and simulated VSWRs of the proposed cavity-backed array with uniform excitation is below 2 over 5:1 bandwidth as seen in Fig. 13. The ripple in the measured results is due to the coaxial cables not present in the model.

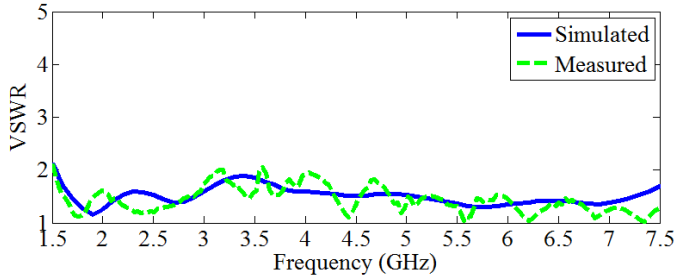


Fig. 13. Measured and simulated VSWRs of the unifromely-excited cavity-backed array.

The measured and simulated broadside gain and the theoretical gain of a uniformly-excited aperture antenna of identical aperture size as the cavity are plotted in Fig. 14. As seen, measured gain is similar to the gain of the uniformly excited aperture antenna from 2.5 to 7.5 GHz. It can also be observed that the proposed array has higher gain than the uniformly-excited aperture at low frequencies. This is due to the fringing fields which contribute to the increased electrical size of the aperture at these frequencies. Gain above 5dBi is obtained at 1.5GHz, and its value increases monotonically over the operating band reaching 15dBi at 7.5GHz. The aperture efficiency of the proposed configuration shown in Fig. 15 is > 80% over most of the bandwidth. This high aperture efficiency is a result of the combined effect of the tightly-coupled Vivaldi array and the cavity where the proposed arrangement creates a nearly uniform aperture illumination. The aperture efficiency is also seen to be >100% at lower frequencies due to the fringing fields contributing to increase the electrical size of the aperture.

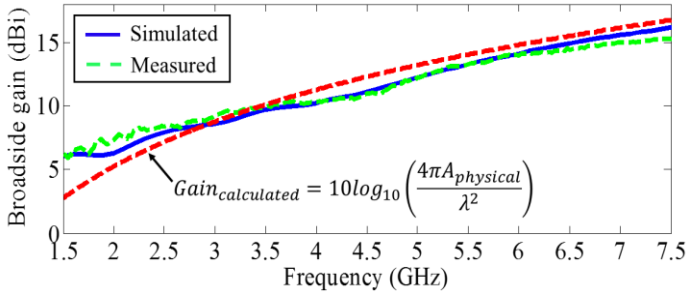


Fig. 14. Measured and simulated gain of the proposed array. The gain is compared to the gain of a uniformly-excited aperture antenna with identical aperture size.

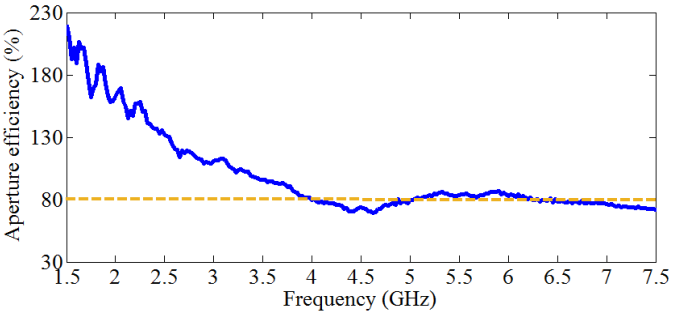


Fig. 15. Aperture efficiency of the proposed antenna calculated with respect to a physical aperture of 60× 100mm$^2$.

The measured and simulated E- and H-plane radiation patterns are plotted in Fig. 16. Patterns are symmetric with SLL < -20dB and low cross polarization characterized with cross polarization discrimination (XPD) of >25dB over the desired band. The demonstrated agreement between the measurement and simulation indicates the effectiveness and quality of the used low-cost fabrication approach and the robustness of the developed design.

This article has been accepted for publication in a future issue of this journal, but has not been fully edited. Content may change prior to final publication. Citation information: DOI 10.1109/TAP.2017.2775286, IEEE Transactions on Antennas and Propagation



## V. Discussion

The scanning VSWR and radiation patterns of the proposed cavity-backed Vivaldi array are synthesized from the measured S-parameters and patterns of the active elements.

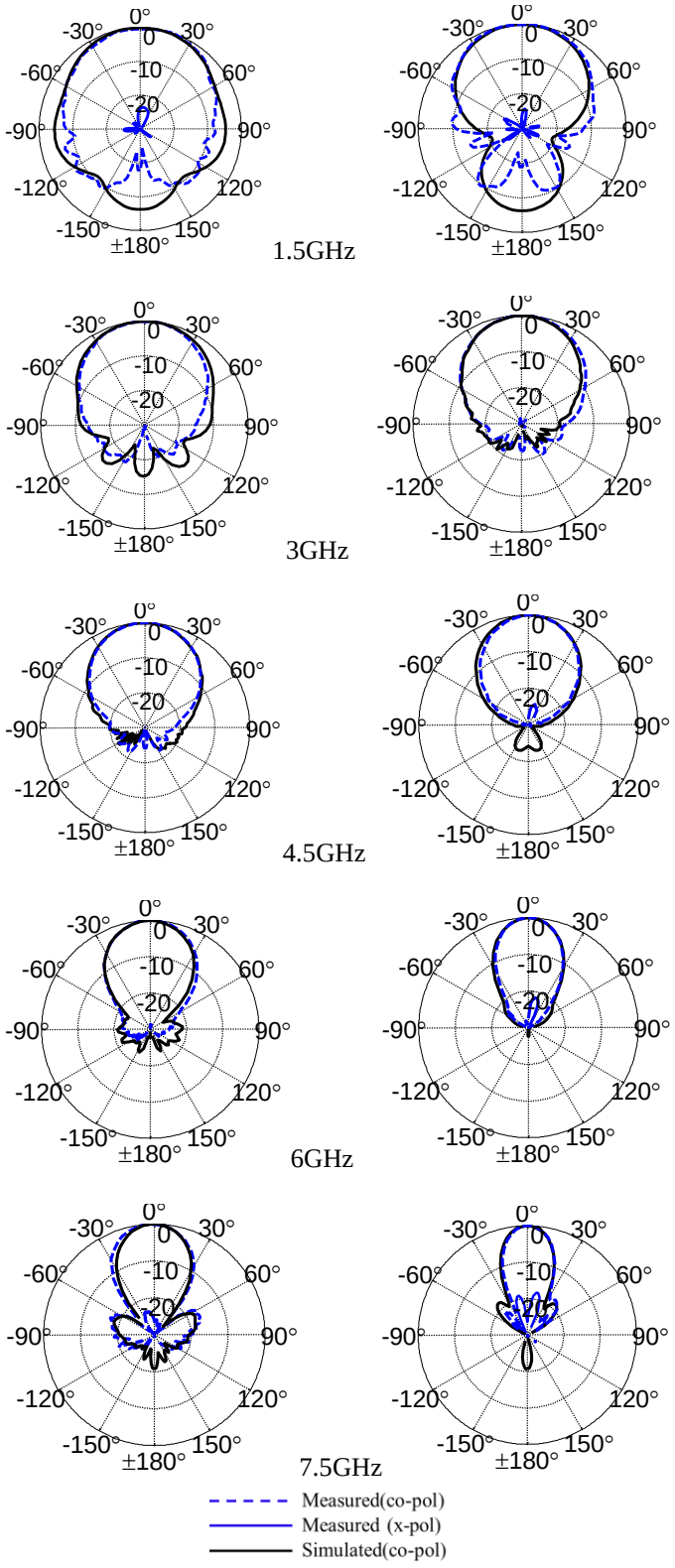


Fig. 16. Measured and simulated broadside radiation patterns of the 3×4 cavity-backed array in (left) E-plane, and (right) H-plane.

The performance is then compared to that of a free-standing counterpart to demonstrate that the proposed cavity-backing approach does not significantly degrade the scanning performance. Notice that the proposed array is designed mainly for non-scanning broadside radiation and its scanning performance can be improved by several approaches, such as mutual coupling compensation techniques [26]-[27]. For the purpose of simplicity of the proposed analysis, conventional phased tapering is used in this study [28].

The free-standing 3×4 Vivaldi array is shown in Fig. 17 with its center and two H-plane edge elements highlighted. For the purpose of this analysis, the active VSWR at the center element and the input VSWR are compared to the proposed cavity-backed array when scanned at 45° in E-plane. The input VSWR is defined here as the VSWR measured at the input of a practical corporate feed network. These VSWRs are shown in Fig. 18 for 45° scan. As seen, the active VSWR of the cavity-backed array is < 3 over most of the band. The active VSWR of the simulated cavity-backed array is also seen to compare well with free-standing antenna. Some spikes due to experimental non-idealities are observed in the measured active VSWR. Nonetheless, the overall response follows a trend similar to the simulated antenna. The measured input VSWR for 45° scan is also shown to be less than 2 over the entire band. While the active VSWR may be considered high, the input VSWR is seen to be very low. This is due to the active cancellation of the combined S-parameters. In practical realization, this return power will be dissipated inside the feed network or reradiated.

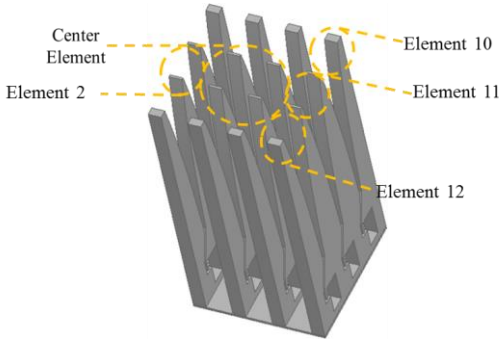


Fig. 17. Illustration of the free-standing 3×4 array with highlighted edge and center elements.

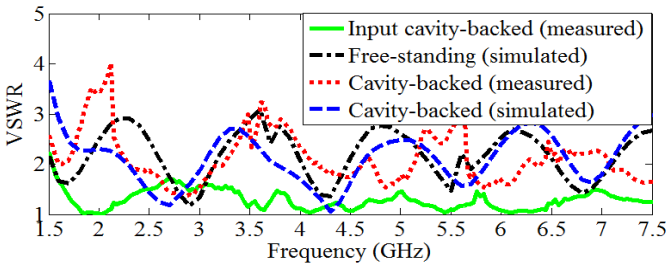


Fig. 18. Synthesized measured input VSWR, central element active VSWR of the cavity-backed and free standing arrays when scanned at 45° in E-plane.

The array mismatch efficiency [29], calculated in (5) for N-element array is another figure of merit often used to assess the percentage of power globally accepted by the array. $S_{p,p}$ in (5) is the active reflection coefficient of element $p$.

This article has been accepted for publication in a future issue of this journal, but has not been fully edited. Content may change prior to final publication. Citation information: DOI 10.1109/TAP.2017.2775286, IEEE Transactions on Antennas and Propagation



$$\varepsilon = \left( N - \sum_{p=1}^{p=N} \left| S_{p,p} \right|^2 \right) \Big/ N \qquad (5)$$

The total mismatch performance of the array for 45° scan in both E- and H-planes is shown in Fig. 19. The cavity-backed array is seen to have similar mismatch efficiency as the free-standing array for E-plane scanning. The efficiency is >70% below 4GHz and remains >80% for higher frequencies. Similar observation is made for H-plane scanning above 3GHz. The efficiency is also seen to be more degraded at low frequencies for H-plane scanning (Fig. 19 (b)). This degradation is mainly due to the edge elements. The interaction between these elements and the array is stronger at lower frequencies. Also the inherent broadside radiation of the cavity contributes to the degradation observed in the VSWR response at low frequencies. Nonetheless, the value of mismatch efficiency for 45° scan is only 10% lower than efficiency obtained for broadside radiation as shown in Fig. 19 (c). It is observed that for broadside radiation, the cavity-backed array has an overall better mismatch efficiency than the free standing array composed of identical number of elements. This improvement in efficiency is attributed to the addition of coherent radiation in broadside direction by the cavity for uniformly excited array.

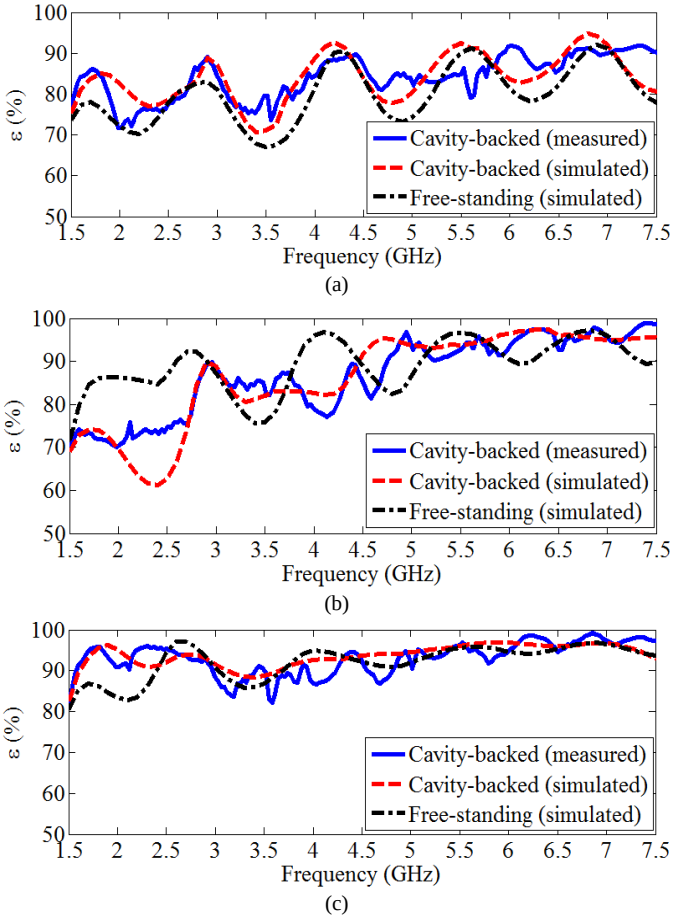


Fig. 19. Array mismatch efficiency for (a) 45° scan in E-plane, (b) 45° scan in H-plane, and (c) broadside radiation.

The measured and simulated radiation patterns of the free-standing and cavity-backed arrays at 7GHz when scanned to 45° in both E- and H-planes are shown in Fig. 20(a) and (b). As seen, the patterns of the cavity-backed array are similar to those of the free-standing case. This indicates that the scan performance of the array is mantained when the array is recessed and properely integrated with the cavity. One should however notice that the first side-lobe of the cavity-backed array is higher than in the free-standing case. This is more pronounced for the H-plane scanning as seen in Fig. 20(a). The side-lobe level increase is attributed to the cavity interaction which radiates mainly in broadside radiation and does not obey the scan requirement imposed on the array elements. The side lobe level can be reduced by modifying array excitation, more precisely, the excitation of elements closer to the cavity. To illustrate this, the scan pattern of the cavity-backed array at 45° scan in the H-plane is shown in Fig. 21(a) with elements 2 and 11 of Fig. 17 not excited, and in Fig. 21(b) with elements 10 and 12 not excited. Element 2 and 11 are the two edge elements not connected to the cavity, while elements 10 and 12 are the edge elements directly connected to the cavity. As seen, about 2 to 4.6dB reduction in sidelobes is observed for Fig. 21(a). The sidelobe levels are seen to improve by more than 4.5 dB in Fig. 21(b) when elements 10 and 12 are connected to the cavity. Not exciting these elements modifies the aperture field and reduces the surface currents on the cavity. The low radiation of these currents along with the modified array excitation result in the reduction seen in the sidelobe level. This preliminary analysis sustantiates the fact that the scan perforamance of the proposed cavity-backed array can be further improved by using a non-conventional excitation taper [28].

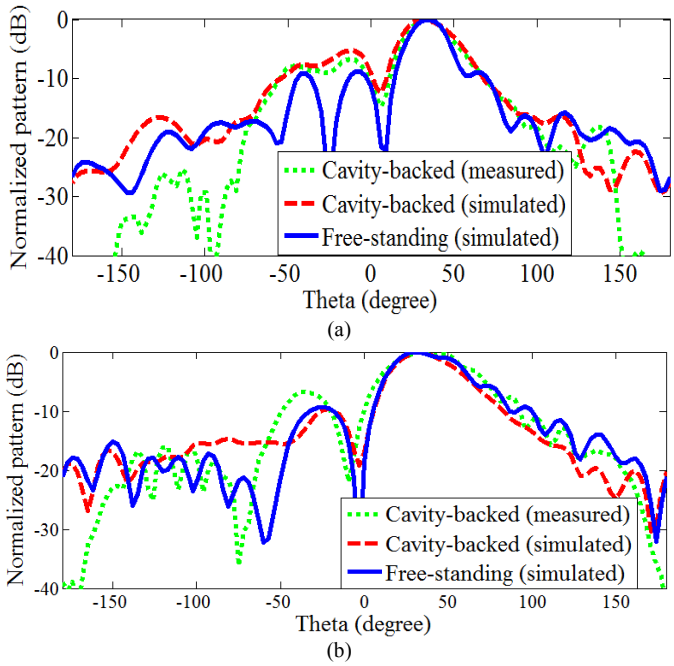


Fig. 20. Measured and simulated radiation patterns of the 3×4 free-standing and cavity-backed Vivaldi arrays at 7 GHz when scanned at (a) 45° in H-plane, and (b) 45° in E-plane.

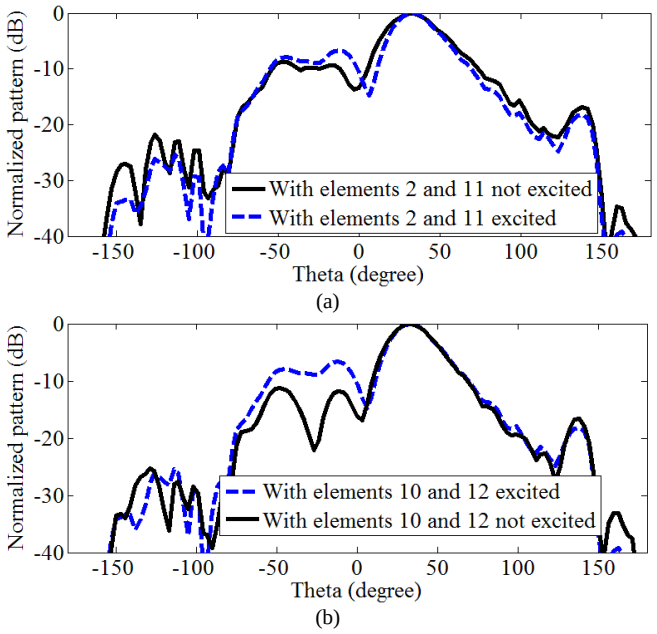


Fig. 21. Measued radiation patterns of the 3×4 cavity-backed Vivaldi arrays when scanned to 45° in H-plane at 7GHz with (a) elements 2 and 11 of Fig. 17 not excited, and (b) elements 10 and 12 of Fig. 17 not excited.

## VI. Conclusion

A multi-octave performance of a Vivaldi array is demonstrated after recessing it inside a metallic enclosure. It is seen that if a proper care is taken when recessing this radiator inside a cavity, excitation of resonant modes may be avoided. The proposed all-metal antenna does not use absorbing materials and yet exhibits resonance-free behavior over 5:1 bandwidth. The cost-effective prototyping has shown to have minor effect on antenna performance. VSWR < 2, gain > 5dBi, and low side lobes with symmetric patterns are demonstrated. Favorable agreement with the theory verifies the robustness of the proposed design. Initial investigation of antenna scan capabilities demonstrates comparable performance with its free space counterpart.

## References

[1] M. Jones and J. Rawnick, "A new approach to broadband array design using tightly coupled elements," *in Proc. IEEE Military Communications Conf*., pp. 1–7, Oct. 2007.

[2] J. Doane, K. Sertel, and J. Volakis, "A wideband, wide scanning tightly coupled dipole array with integrated balun (TCDA-IB)," *IEEE Trans. Antennas Propag*., vol. 61, no. 9, pp. 4538–4548, Sep. 2013.

[3] W. F. Moulder, K. Sertel, and J. L. Volakis, "Superstrate-enhanced ultrawideband tightly coupled array with resistive FSS," *IEEE Trans. Antennas Propag*., vol. 60, no. 9, pp. 4166–4172, Sep. 2012.

[4] S. S. Holland, D. H. Schaubert, and M. N. Vouvakis, "A 7-21GHz dualpolarized planar ultrawideband modular antenna (PUMA) array," *IEEE Trans. Antennas Propag*., vol. 60, no. 10, pp. 4589–4600, Jul. 2012.

[5] S. S. Holland and M. N. Vouvakis, "The planar ultrawideband modular antenna (PUMA) array," *IEEE Trans. Antennas Propag.*, vol. 60, no. 1, pp. 130–140, Sep. 2012

[6] B. A. Munk, Finite Antenna Arrays and FSS. New York, NY, USA:Wiley, 2003.

[7] E. Irci, K. Sertel, and J. Volakis, "Bandwidth enhancement of low-profile microstrip antennas using tightly coupled patch arrays," *in Proc. IEEE Antennas Propag. Soc. Int. Symp. (APSURSI)*, Spokane, WA, Jul. 2011.

[8] D. H. Schaubert , S. Kasturi , A. O. BoryssenkoI, and W. M. Elsallal, "Vivaldi antenna arrays for wide bandwidth and electronic scanning," *in Proc. Eur. Conf. Antennas Propag. (EuCAP)*, Edinburgh, UK, pp. 1–6, Nov. 2007.

[9] R. W. Kindt and W. R. Pickles, "Ultrawideband all-metal flared-notch array radiator," *IEEE Trans. Antennas Propag*., vol. 58, no. 11, pp. 3568-3575, Nov. 2010.

[10] J. D. S. Langley, P. S. Hall, and P. Newham, "Novel ultrawide-bandwidth Vivaldi antenna with low crosspolarization," *Electron. Lett*., vol. 29, pp. 2004–2005, Nov. 1993.

[11] P. Dixon, "Cavity-resonance dampening," *IEEE Microw. Mag*., vol. 6, no. 2, pp. 74–84, Jun. 2005.

[12] S. W. Qu, J. L. Li, Q. Xue, and C. H. Chan, "Wideband cavity-backed bowtie antenna with pattern improvement," *IEEE Trans. Antennas Propag.*, vol. 56, no. 12, pp. 3850–3854, Dec. 2008.

[13] R. A Moddy and S.K Sharma,"Ultra-wide Bandwidth Planar Monopole Antenna Backed by Novel Pyramidal-Shaped Cavity Providing Directional Radiation Patterns," *in IEEE Antennas Wireless Propag. Lett*, pp.1469–1472, Dec. 2011.

[14] D. Awan, S. Bashir, and W. Whittow, "High gain cavity backed UWB antenna with and without band notch feature," *in Proc. IEEE Antennas Propag. Conf. (LAPC)*, Loughborough, UK, Nov. 2013.

[15] M. OstadRahimi, L. Shafai, and J. Lovetri, "Analysis of a doubled-layered Vivaldi antenna inside a metallic enclosure", *Prog In Electromag Resarch*., vol. 143, pp. 503–518, Nov. 2013.

[16] M. Abbak, M. Cayoren, and I. Akduman,"Microwave breast phantom measurements with a cavity-backed Vivaldi antenna", *IET Microwaves, Antennas Propag*., vol. 8, pp. 1127–113, Oct. 2014.

[17] A. Tibaldi, et al., "Design considerations for a low frequency Vivaldi array element," *in PIERS Proc*, Stockholm, Sweeden, pp. 240–244, Aug. 2013.

[18] D. G. Lopez and D. S. Filipovic, "Flush mountable K/Ka band amplitude only direction finding system," *in Proc. IEEE Antennas Propag. Soc. Int. Symp. (APSURSI)*, Fajardo, Puerto Rico, Jun. 2016.

[19] E. Tianang, M. Elmansouri, and D. S. Filipovic, "Cavity-backed Vivaldi array antenna," *in Proc. Eur. Conf. Antennas Propag. (EuCAP)*, Davos, Switzerland, Apr. 2016.

[20] E. Tianang, M. Elmansouri, and D. S. Filipovic, "Flush-mountable Vivaldi array antenna," *in Proc. IEEE Antennas Propag. Soc. Int. Symp. (APSURSI)*, Fajardo, Puerto Rico, Jun. 2016.

[21] N. Jastram and D. S. Filipovic, "Wideband millimeter-wave surface micromachined tapered slot antenna," *IEEE Antennas Wireless Propag. Lett.*, vol. 13, no. 1, pp. 285–288, Jan. 2014.

[22] B. T. McWhirter, S. K. Panaretos, J. Fraschilla, L.R. Walker, and J.L.Edie, "Thick flared notch radiator array," U.S. patent 5 659 326, Aug. 19, 1997.

[23] M. Lukic, S. Rondineau, Z. Popovic, and D. S. Filipovic, "Modeling of realistic rectangular $\mu$-coaxial lines," *IEEE Trans. Microw. Theory Tech.*, vol. 54, no. 5, pp. 2068–2076, May 2006.

[24] A. K. Bhattacharyya, "*Phased Array Antennas, Floquet analysis, synthesis, BFNs, and active array systems*," John Willey & Sons, Inc. Hoboken, New Jersey, 2006.

[25] ANSYS High Frequency Structure Simulation (HFSS), Version 15.0.0.

[26] P. Darwood, P. N. Fletcher, and G.S. Hilton, "Mutual coupling compensation in small planar array antennas," *IEE Proc.-Micro. Antennas Propagat.*, vol. 145, no. 1, pp. 1–6, Feb. 1998

[27] H. Steyskal and J. S. Herd, "Mutual coupling compensation in small array antennas," *IEEE Trans. Antennas Propag*., vol. 38, no. 12, pp. 1971–1975, Dec. 1990.

[28] R. C. Hansen, *Phased Array Antennas*, New York; Wiley-Interscience, 1998.

[29] R. W. Kindt and M. N. Vouvakis, "Analysis of a wavelength-scaled array (WSA) architecture," *IEEE Trans. Antennas Propag.*, vol. 58, no.9, pp. 2866–2874, Sep. 2010.